Characterizing aqueous solution conformations of a peptide backbone using Raman optical activity computation

Parag Mukhopadhyay, Gérard Zuber, and David N. Beratan

Departments of Chemistry and Biochemistry,

Duke University

5311 French Family Science Center, Durham, North Carolina 27708, U.S.A

Fax: (+) 919-660-1605

E-mail: gzuber@duke.edu; david.beratan@duke.edu

Supporting Information

1. Structures of Ala dipeptide-H_2O clusters

Figure S1A shows the Ramachandran map for Ala dipeptide structures taken from the MC simulations prior to geometry optimization (see computational methods in the manuscript for detail). Each ϕ, ψ pair (black) represents a cluster of H_2O-Ala dipeptide cluster that have the same peptide backbone dihedral angles with different water geometries. The ϕ, ψ values correspond to peptide geometries from low-energy regions 1, 2, and 3 of the Ramchandran map (Figure S1A). The ϕ, ψ values for H_2O-Ala dipeptide structures, and the number of structures for each ϕ, ψ pair, appear in Table 1 (360 total structures). Figure S1B shows a wider distribution of ϕ, ψ values for the structures of H_2O-Ala dipeptide clusters, optimized using quantum mechanical energy minimization. The peptide backbone dihedral angles changes upon geometry optimization. However, each peptide conformation, before and after geometry optimization, occupies the same region of the Ramachandran map. Following geometry optimization of the H_2O-Ala dipeptide cluster, the structures were used for computing ROA and Raman spectra using time-dependent DFT.

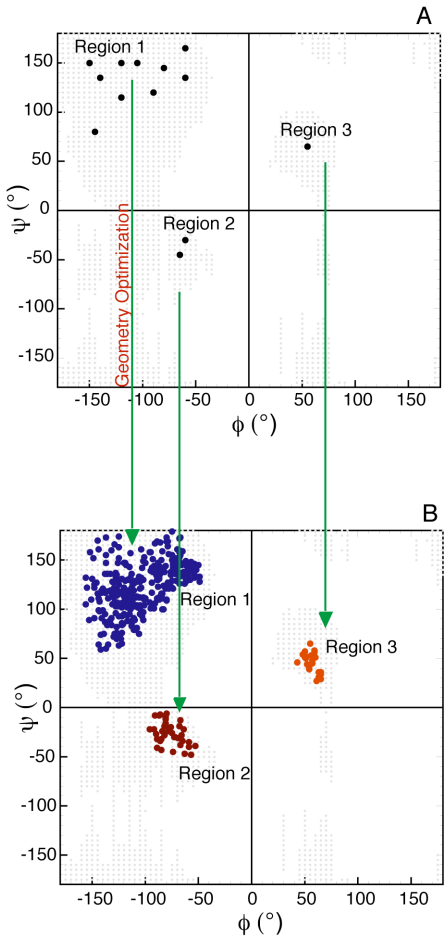

Figure S1. Ramachandran map of ϕ, ψ pairs for Ala dipeptide-water cluster structures taken from the Monte Carlo simulations. Figure S1A shows a collection of Ala dipeptide-water cluster structures (black) that have the same peptide backbone conformation with different water arrangements. Figure S1B shows the distribution of ϕ, ψ values for the alanine dipeptide-water clusters optimized using quantum mechanical energy minimization. Green arrows show that each peptide conformation, before and after energy minimization, occupies the same region on the Ramachandran map.

Table 1. The peptide backbone dihedral angles (ϕ, ψ) of alanine dipeptide-water cluster structures from the Monte Carlo simulations used in the quantum mechanical energy minimization.

ϕ, ψ values (deg)	Number of structures with explicit water
-150, 150	30
-140, 135	30
-120, 115	30
-90, 120	30
-120, 150	30
-105, 150	30
-80, 145	30
-60, 165	30
-60, 135	30
-145, 80	30
-65, -45	20
-60, -30	10
55, 65	30

2. Dependence of computed ROA spectra on the ϕ, ψ dihedral angles of Ala dipeptide-H_2O clusters

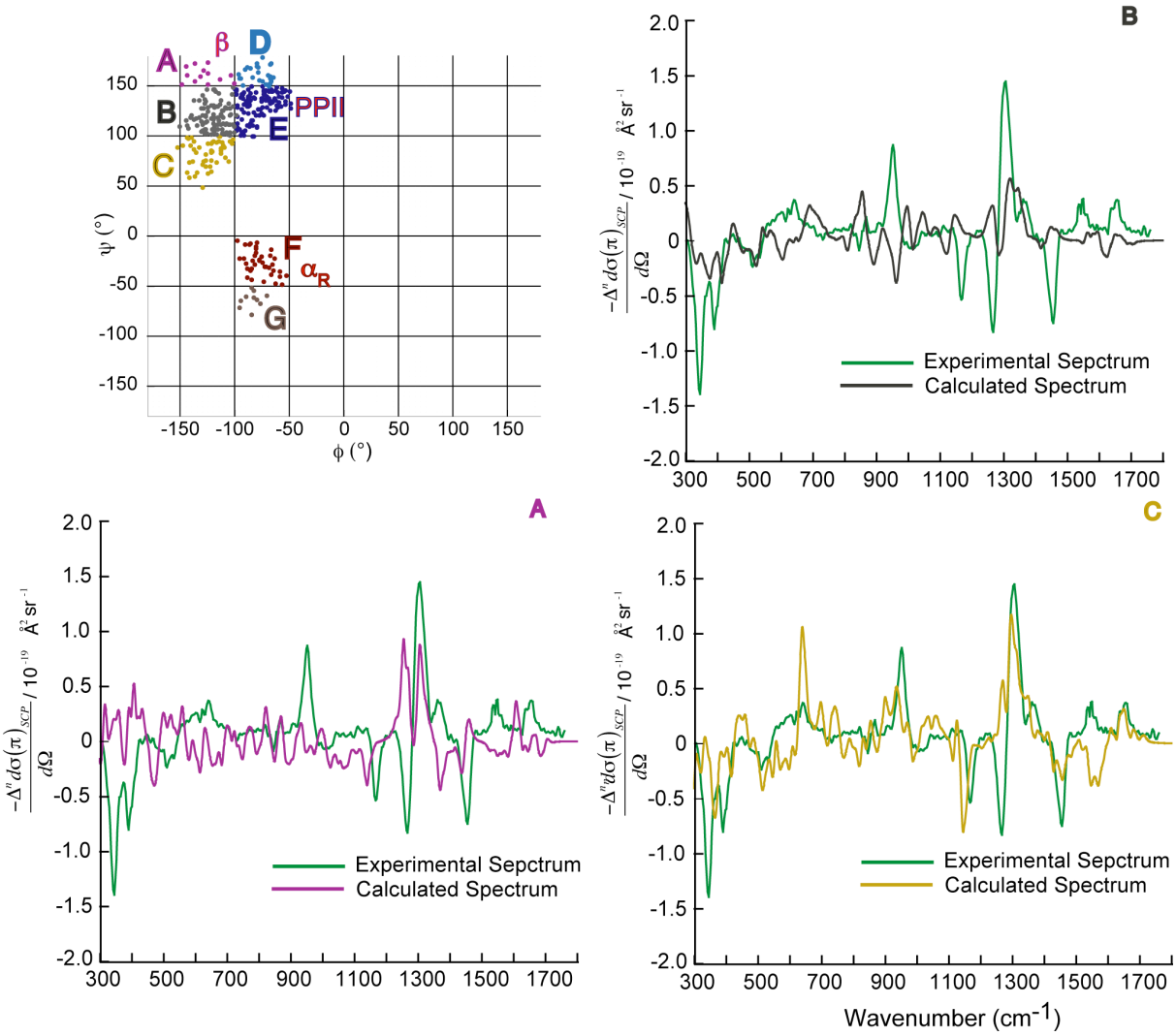

Figure S2. ROA spectra computed using Ala dipeptide-H_2O cluster from the low-energy region of the Ramachandran map. The computed spectra shown are averaged over a collection of dipeptide conformations from regions A, B and C of the Ramchandran map (inset in A). The experimental spectrum (in arbitrary units) is from reference [14].

Figures S2 and S3 show the computed ROA spectra for Ala dipeptide-water cluster from the low-energy regions of the Ramchandran map. For example, Figures S2A, S3E and S3F show the computed ROA spectra using sets of Ala dipeptide conformations from the β, PPII and α_R conformational region of the Ramchandran map (insets in Figures S2 A, E and F), respectively. The computed spectra are averaged over sets of Ala dipeptide conformations on 50° × 50° grids of ϕ and ψ.

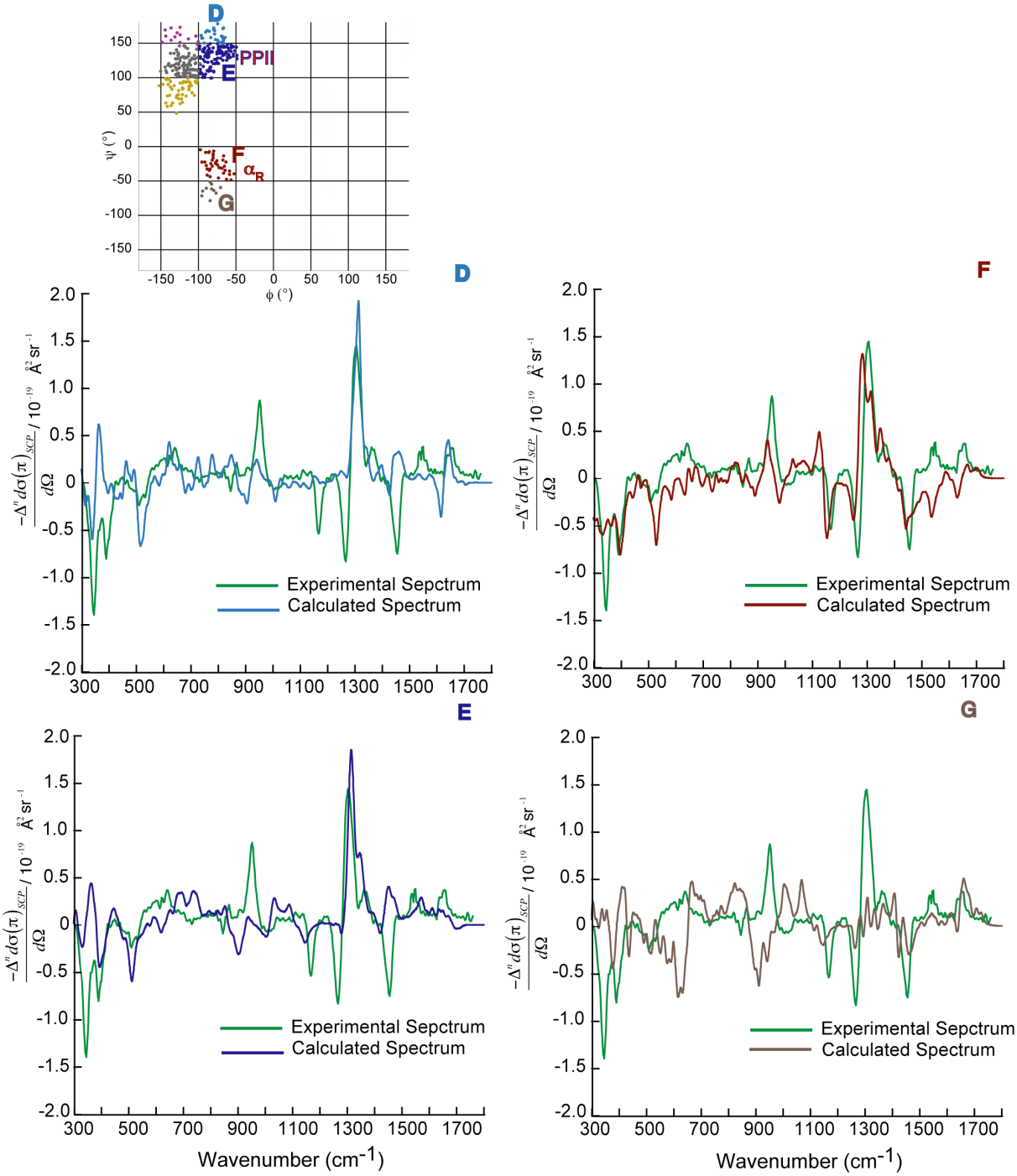

Figure S3. ROA spectra computed using Ala dipeptide-H_2O cluster from the low-energy region of the Ramachandran map. The computed spectra shown are averaged over a collection of dipeptide conformations from regions D, E, F and G of the Ramchandran map (inset in A). The experimental spectrum (in arbitrary units) is from reference [14].

The ROA spectral features in the computed spectra using PPII (Figure S3E), α_R (Figure S3F) and β (Figure S2A) conformations of Ala dipeptide in aqueous solution are very different. Thus, different ROA spectrum originates from very different peptide conformations, and hence a conformational preference of a peptide is obtained by correlating simulated and measured ROA spectra of the peptide in aqueous solution.

3. Dependence of computed ROA spectra on the ϕ, ψ dihedral angles of Ala dipeptide-D_2O clusters

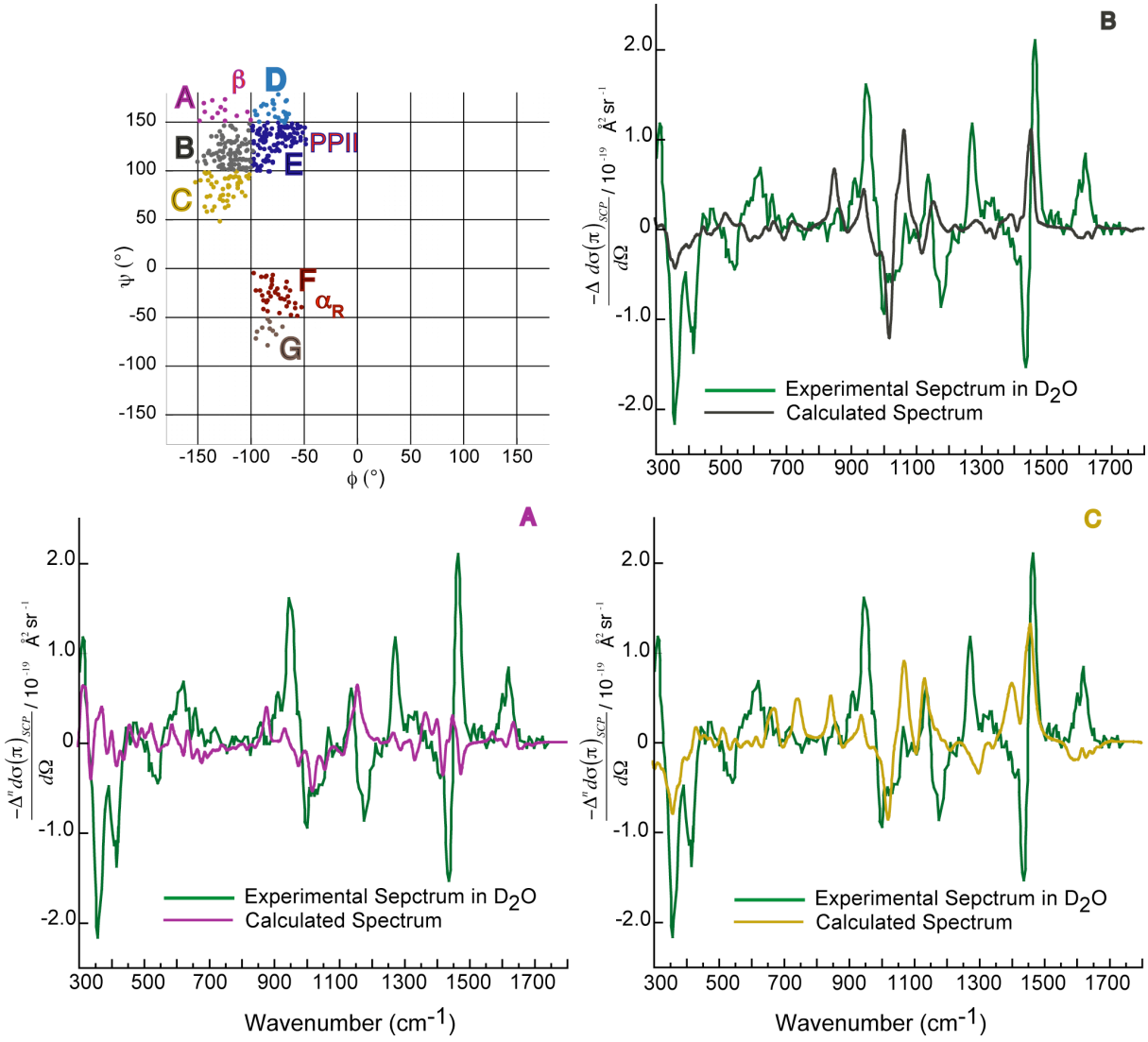

Figure S4. ROA spectra computed using Ala dipeptide-D_2O cluster from the low-energy region of the Ramachandran map. The computed spectra shown are averaged over a collection of dipeptide conformations from regions A, B and C of the Ramchandran map (inset in A). The experimental spectrum (in arbitrary units) is from reference [14].

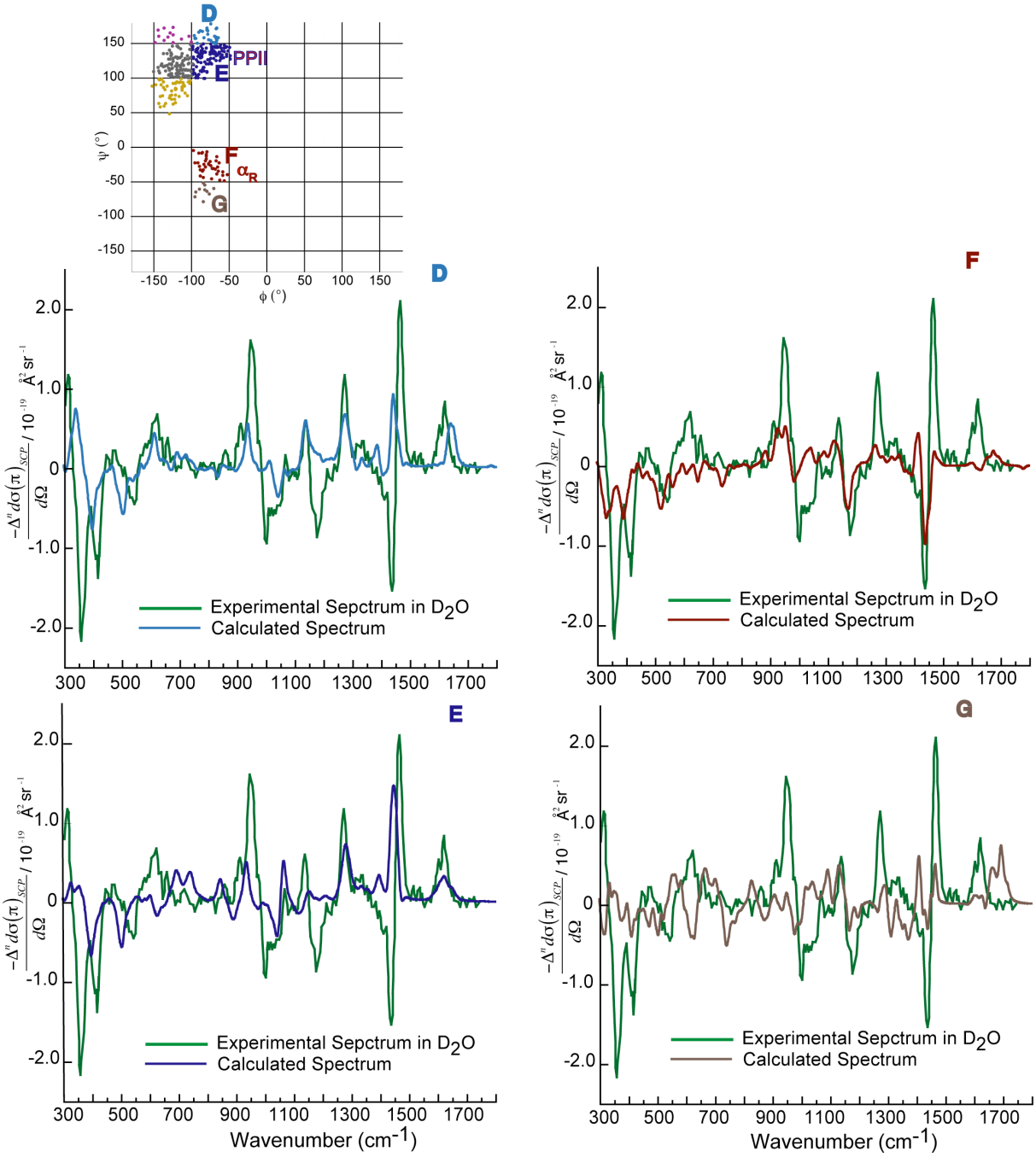

Figure S5. ROA spectra computed using Ala dipeptide-D_2O cluster from the low-energy region of the Ramachandran map. The computed spectra shown are averaged over a collection of dipeptide conformations from regions D, E, F and G of the Ramchandran map (inset in A). The experimental spectrum (in arbitrary units) is from reference [14].

Figures S4 and S5 both show the dependence of the computed ROA spectra on the ϕ and ψ angles of Ala dipeptide in D_2O. For example, the ROA spectral features in the computed spectra using PPII (Figure S5E), α_R (Figure S5F) and β (Figure S4A) conformations of Ala dipeptide in aqueous solution are very different. Thus, similar to the H_2O results, different ROA spectrum originates from very different peptide conformations, and hence a conformational preference of a peptide is obtained by correlating simulated and measured ROA spectra of the peptide in aqueous solution.

4. ROA spectra of the H_2O- and D_2O-Ala dipeptide clusters from the α_L and β regions of the Ramachandran map.

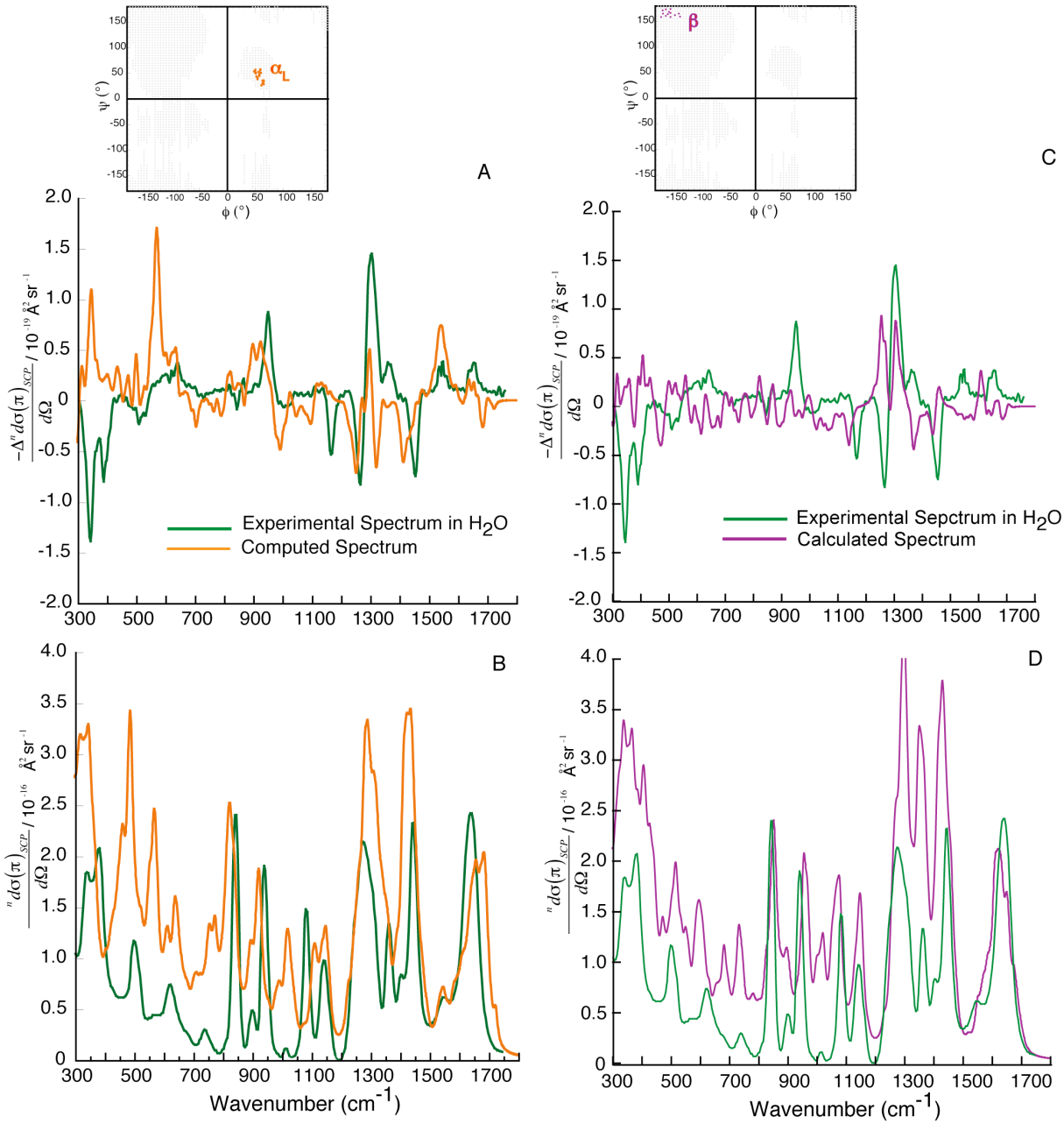

Figure S6. SCP backscattering ROA (A, C) and Raman (B, D) spectra of Ala dipeptide in H_2O. The computed spectra shown in orange and pink are averaged over a collection of dipeptide conformations from α_L (inset in A) and β (inset in C) regions of the Ramchandran map. The experimental spectrum (in arbitrary units) is from reference [14].

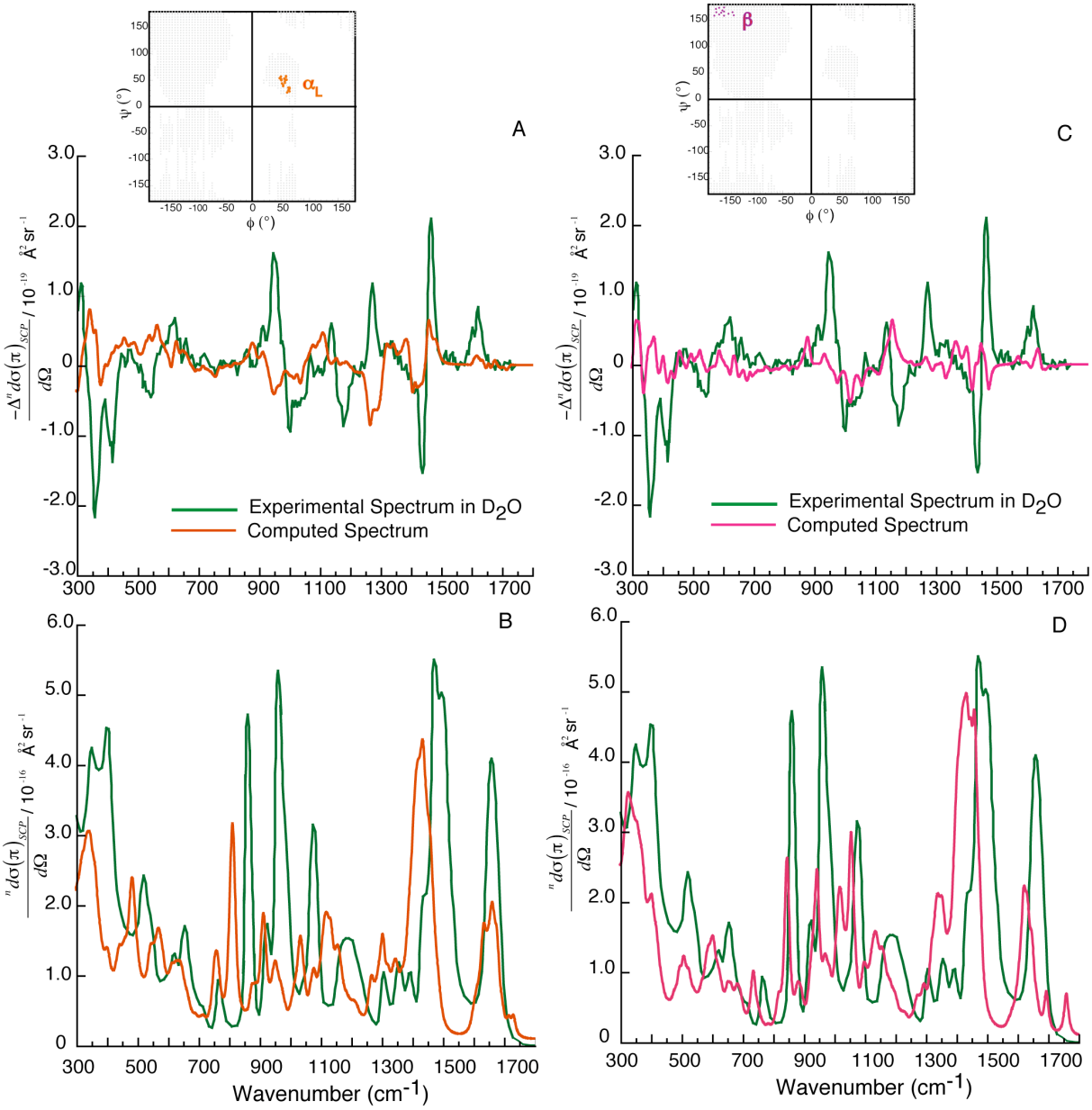

Figure S7. SCP backscattering ROA (A, C) and Raman (B, D) spectra of Ala dipeptide in D_2O. The computed spectra shown in orange and pink are averaged over a collection of dipeptide conformations from α_L (inset in A) and β (inset in C) regions of the Ramchandran map. The experimental spectrum (in arbitrary units) is from reference [14].

Figures S6 and S7 show that there is no significant correlation between the measured and computed ROA and Raman spectra using the α_L (with $45° \leq \phi \leq 65°$ and $25° \leq \psi \leq 55°$) and β (with $-180° \leq \phi \leq -125°$ and $150° \leq \psi \leq 180°$) conformations of H_2O-Ala dipeptide and D_2O-Ala dipeptide clusters. Thus, ourROA analysis suggests that Ala dipeptide in water populates α_R and PPII conformations but no substantial population of α_L and β structures.

5. Group coupling matrices for the Raman intensities associated with the vibrations in the low wavenumber for a PPII a α_R of Ala dipeptide.

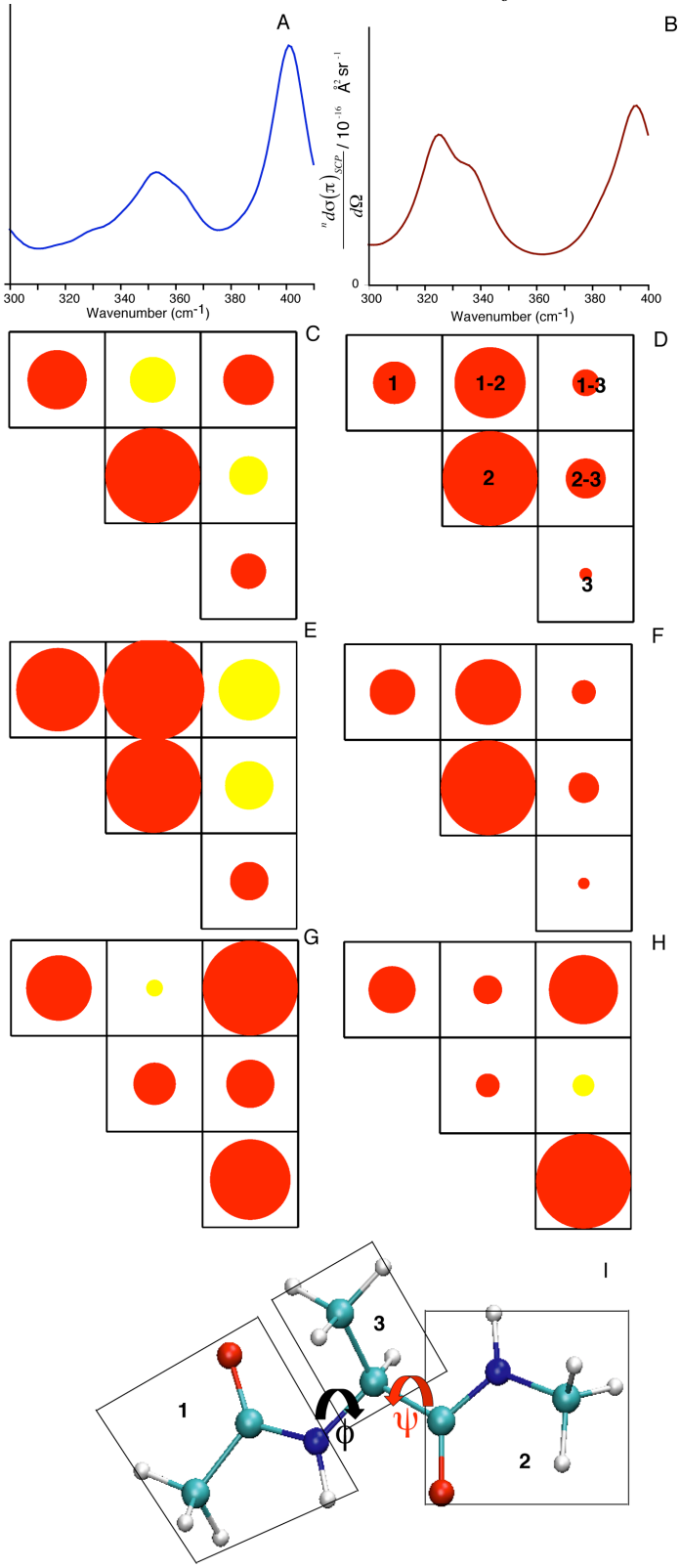

Figure S8. Raman intensity differences associated with the vibrations in the low wavenumber range decomposed into contributions from groups of atoms in Ala dipeptide for a PPII (ϕ = -68° and ψ = 135°; A) and a α_R (ϕ = -73° and ψ = −30°; B) conformation. Positive and negative Raman intensity differences are shown as red and yellow circles. The groups of atoms corresponding to the matrix elements are shown in I.

Figures S8 C and G shows the Raman intensities associated with the vibrations at ~364 cm^{-1}(C) and at ~401 cm^{-1} (G) for a PPII conformation of Ala dipeptide. Similarly, Figures S8 D and H shows the group coupling matrices for the Raman intensities associated with the vibrations at ~325 cm^{-1}(D) and at ~395 cm^{-1} (H) for a α_R (ϕ = -73° and ψ = −30) conformation of Ala dipeptide. Figures S8 E and F show the ROA intensity differences associated with molecular vibrations at ~352 cm^{-1} for the PPII and at ~338 cm^{-1} for the α_R conformation.

References

(1) Jorgensen, W. L.; Tirado-Rives, J. *J. Comput. Chem.* **2005**, *26*, 1689.

(2) Allen, M. P.; Tildesley, D. J. In *Computer simulations of liquids*; Oxford University Press: Oxford, 1987.

(3) Jorgensen, W. L.; Maxwell, D. S.; TiradoRives, J. *J. Am. Chem. Soc.* **1996**, *118*, 11225.

(4) Jorgensen, W. L.; Chandrasekhar, J.; Madura, J. D.; Impey, R. W.; Klein, M. L. *J. Chem. Phys.* **1983**, *79*, 926.

(5) Dewar, M. J. S.; Zoebisch, E. G.; Healy, E. F.; Stewart, J. J. P. *J. Am. Chem. Soc.* **1985**, *107*, 3902.

(6) Storer, J. W.; Giesen, D. J.; Cramer, C. J.; Truhlar, D. G. *J. Comput-Aided Mol. Des.* **1995**, *9*, 87.

(7) (a) Zuber, G.; Goldsmith, M. R.; Beratan, D. N.; Wipf, P. *Chemphyschem* **2005**, *6*, 595. (b) Luber, S.; Herrmann, C.; Reiher, M. *J. Phys. Chem. B* **2008**, *112*, 2218.

(8) Barron, L. D.; Buckingh.Ad. *Mol. Phys.* **1971**, *20*, 1111.

(9) Barron, L. D.; Escribano, J. R. *Chem, Phys.* **1985**, *98*, 437.

(10) Hug, W. *Chem. Phys. Lett.* **2001**, *264*, 53.

(11) Ahlrichs, R.; Bär, M.; Baron, H.-P.; Bauernschmitt, R.; Böcker, S.; Ehrig, M.; Eichkorn, K.; Elliott, S.; Furche, F.; Haase, F. e. a. Turbomole 5.6, 2002.

(12) Eichkorn, K.; Weigend, F.; Treutler, O.; Ahlrichs, R. *Theor. Chem. Acc.* **1997**, *97*, 119.

(13) Grimme, S.; Furche, F.; Ahlrichs, R. *Chem. Phys. Lett.* **2002**, *361*, 321.

(14) Deng, Z.; Polavarapu, P. L.; Ford, S. J.; Hecht, L.; Barron, L. D.; Ewig C. S.; Jalkanen, K. *J. Phys. Chem.* **1996**, 100, 2025.